The "fireshell" model and the "canonical" GRB scenario.

Carlo Luciano Bianco[*,†], Maria Grazia Bernardini[*,†], Letizia Caito[*,†], Maria Giovanna Dainotti[*,†], Roberto Guida[*,†] and Remo Ruffini[*,†]

[*]ICRANet, Piazzale della Repubblica 10, 65122 Pescara, Italy.
[†]Dipartimento di Fisica, Università di Roma "La Sapienza", Piazzale Aldo Moro 5, 00185 Roma, Italy.

Abstract. In the "fireshell" model we define a "canonical GRB" light curve with two sharply different components: the Proper-GRB (P-GRB), emitted when the optically thick fireshell of electron-positron plasma originating the phenomenon reaches transparency, and the afterglow, emitted due to the collision between the remaining optically thin fireshell and the CircumBurst Medium (CBM). We outline our "canonical GRB" scenario, originating from the gravitational collapse to a black hole, with a special emphasis on the discrimination between "genuine" and "fake" short GRBs.

INTRODUCTION

The observations of GRB 060614 (Gehrels et al. [15], Mangano et al. [17]) challenged the standard GRB classification scheme (Klebesadel [16], Dezalay et al. [13]) in which the gamma events are branched into two classes: "short" GRBs (events which last less than $\sim$ 2s) and "long" GRBs (events which last more than $\sim$ 2s). GRB 060614, indeed, "reveals a first short, hard-spectrum episode of emission (lasting 5 s) followed by an extended and somewhat softer episode (lasting $\sim$ 100 s)": a "two-component emission structure" (Gehrels et al. [15]). Moreover, stringent upper limits on the luminosity of the Supernova possibly associated with GRB 060614 have been established (Della Valle et al. [12], Gal-Yam et al. [14]). Gehrels et al. [15] concluded that "it is difficult to determine unambiguously which category GRB 060614 falls into" and that, then, GRB 060614, due to its "hybrid" observational properties, "opens the door on a new GRB classification scheme that straddles both long and short bursts" (Gehrels et al. [15]).

These observations motivated Norris & Bonnell [19] to reanalyze the BATSE catalog identifying a new GRB class with "an occasional softer extended emission lasting tenths of seconds after an initial spikelike emission" (Norris & Bonnell [19]). In some cases, "the strength of the extended emission converts an otherwise short burst into one with a duration that can be tens of seconds, making it appear to be a long burst" (Norris & Bonnell [19]). Hence, Norris & Bonnell [19] suggested that the standard "long-short" GRB classification scheme "is at best misleading" (Norris & Bonnell [19]).

In the following, we are going to outline our "canonical GRB" scenario (Ruffini et al. [24, 25, 23], Bernardini et al. [3]), where all GRBs are generated by the same "engine": the gravitational collapse to a black hole. We will show that such "hybrid" sources are indeed explainable in terms of a peculiarly small average value of the CircumBurst Medium (CBM) density, compatible with a galactic halo environment (see Bernardini et al. [3, 4]).

THE "FIRESHELL" MODEL

We assume that all GRBs, including the "short" ones, originate from the gravitational collapse to a black hole (Ruffini et al. [25, 23]). The $e^{\pm}$ plasma created in the process of the black hole formation expands as an optically thick and spherically symmetric "fireshell" with a constant width in the laboratory frame, i.e. the frame in which the black hole is at rest. We have only two free parameters characterizing the source, namely:

- $E_{e^{\pm}}^{tot}$: the total energy of the $e^{\pm}$ plasma,
- $B \equiv \dfrac{M_B c^2}{E_{e^{\pm}}^{tot}}$: the $e^{\pm}$ plasma baryon loading,

where M_B is the total baryons' mass (Ruffini et al. [31]). These two parameters fully determine the optically thick acceleration phase of the fireshell, which lasts until the transparency condition is reached and the Proper-GRB (P-GRB) is emitted (Ruffini et al. [25]).

The afterglow emission then starts due to the collision between the remaining optically thin fireshell and the CBM (Ruffini et al. [25], Bianco & Ruffini [6, 7, 8], Ruffini et al. [23]. It clearly depends on the parameters describing the effective CBM distribution:

- n_{cbm}: its density,
- $\mathscr{R} \equiv \dfrac{A_{eff}}{A_{vis}}$: its filamentary structure,
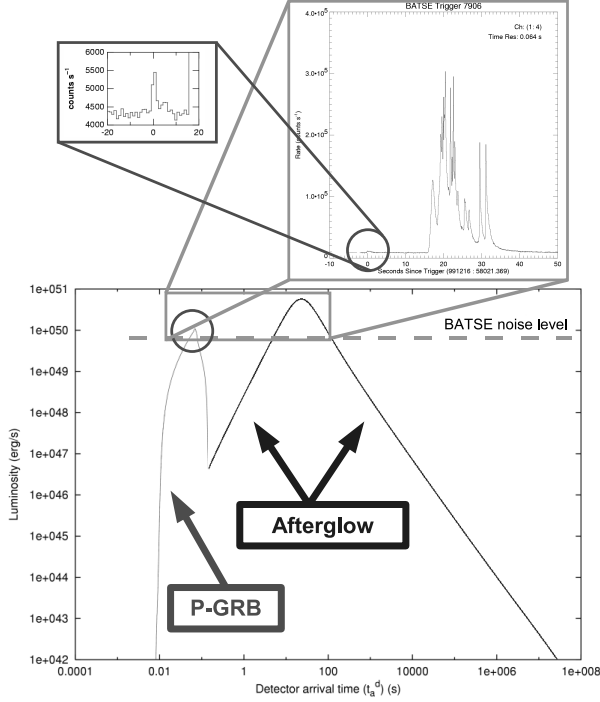
FIGURE 1. The "canonical GRB" light curve theoretically computed for GRB 991216. The prompt emission observed by BATSE is identified with the peak of the afterglow, while the small precursor is identified with the P-GRB. For this source we have $B \simeq 3.0 \times 10^{-3}$ and $\langle n_{cbm} \rangle \sim 1.0$ particles/cm^3. Details in Ruffini et al. [25, 26, 27, 21].

where A_{eff} is the effective emitting area of the fireshell and A_{vis} is its total visible area (Ruffini et al. [26, 28, 29], Dainotti et al. [11]).

THE "CANONICAL" GRB SCENARIO

Unlike treatments in the current literature (see e.g. Piran [20], Mészáros [18] and references therein), we define a "canonical GRB" light curve with two sharply different components (see Fig. 1 and Ruffini et al. [25, 23], Bernardini et al. [3]):

1. **The P-GRB:** it has the imprint of the black hole formation, an harder spectrum and no spectral lag (Bianco et al. [9], Ruffini et al. [30]).
2. **The afterglow:** it presents a clear hard-to-soft behavior (Bernardini et al. [5], Ruffini et al. [28, 22]); the peak of the afterglow contributes to what is usually called the "prompt emission" (see e.g.Ruffini et al. [25, 22], Dainotti et al. [11]).

The ratio between the total time-integrated luminosity of the P-GRB (namely, its total energy) and the corresponding one of the afterglow is the crucial quantity
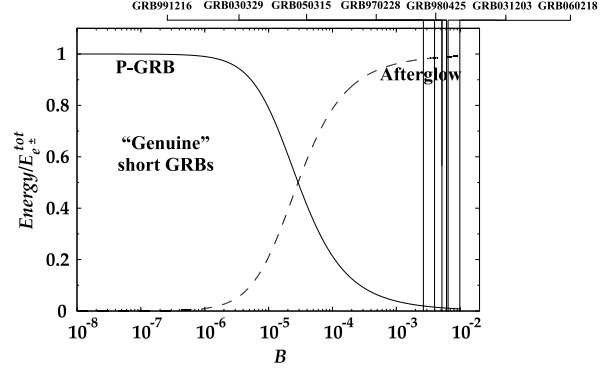

FIGURE 2. The energy radiated in the P-GRB (solid line) and in the afterglow (dashed line), in units of the total energy of the plasma ($E_{e^\pm}^{tot}$), are plotted as functions of the B parameter. Also represented are the values of the B parameter computed for GRB 991216, GRB 030329, GRB 980425, GRB 970228, GRB 050315, GRB 031203, GRB 060218. Remarkably, they are consistently smaller than, or equal to in the special case of GRB 060218, the absolute upper limit $B \lesssim 10^{-2}$ established in Ruffini et al. [31]. The "genuine" short GRBs have a P-GRB predominant over the afterglow: they occur for $B \lesssim 10^{-5}$ (Ruffini et al. [25], Bernardini et al. [3]).

for the identification of GRBs' nature. Such a ratio, as well as the temporal separation between the corresponding peaks, is a function of the B parameter (Ruffini et al. [25]).

When the P-GRB is the leading contribution to the emission and the afterglow is negligible we have a "genuine" short GRB (Ruffini et al. [25]). This is the case where $B \lesssim 10^{-5}$ (see Fig. 2): in the limit $B \to 0$ the afterglow vanishes (see Fig. 2).

In the other GRBs, with $10^{-4} \lesssim B \lesssim 10^{-2}$, the afterglow contribution is generally predominant (see Fig. 2; for the existence of the upper limit $B \lesssim 10^{-2}$ see Ruffini et al. [31] and Dainotti et al. [11]). Still, this case presents two distinct possibilities:

- The afterglow peak luminosity is **larger** than the P-GRB one. A clear example of this situation is GRB 991216, represented in Fig. 1.
- The afterglow peak luminosity is **smaller** than the P-GRB one. A clear example of this situation is GRB 970228, represented in Fig. 3.

The simultaneous occurrence of an afterglow with total time-integrated luminosity larger than the P-GRB one, but with a smaller peak luminosity, is indeed explainable in terms of a peculiarly small average value of the CBM density, compatible with a galactic halo environment, and not due to the intrinsic nature of the source (see Fig. 3 and Bernardini et al. [3, 4]). Such a small average CBM density deflates the afterglow peak luminosity. Of course, such a deflated afterglow lasts much longer,
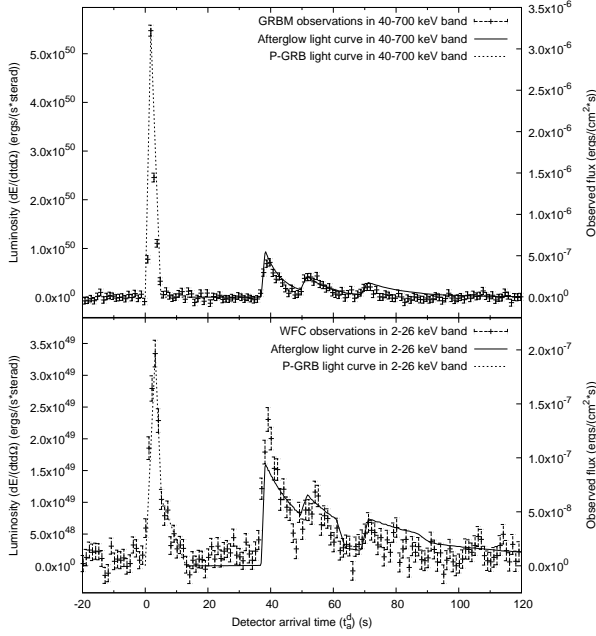
FIGURE 3. The "canonical GRB" light curve theoretically computed for the prompt emission of GRB 970228. *Beppo*SAX GRBM (40–700 keV, above) and WFC (2–26 keV, below) light curves (data points) are compared with the afterglow peak theoretical ones (solid lines). The onset of the afterglow coincides with the end of the P-GRB (represented qualitatively by the dotted lines). For this source we have $B \simeq 5.0 \times 10^{-3}$ and $\langle n_{cbm} \rangle \sim 10^{-3}$ particles/cm^3. Details in Bernardini et al. [3, 4].

since the total time-integrated luminosity in the afterglow is fixed by the value of the *B* parameter (see above and Fig. 4). In this sense, GRBs belonging to this class are only "fake" short GRBs. This is GRB class identified by Norris & Bonnell [19], which also GRB 060614 belongs to, and which has GRB 970228 as a prototype (Bernardini et al. [3, 4], Caito et al. [10]).

CONCLUSIONS

We have presented our "canonical GRB" scenario, especially pointing out the need to distinguish between "genuine" and "fake" short GRBs:

- The **"genuine" short GRBs** inherit their features from an intrinsic property of their sources. The very small fireshell baryon loading, in fact, implies that the afterglow time-integrated luminosity is negligible with respect to the P-GRB one.

- The **"fake" short GRBs**, instead, inherit their features from the environment. The very small CBM density, in fact, implies that the afterglow peak lu-
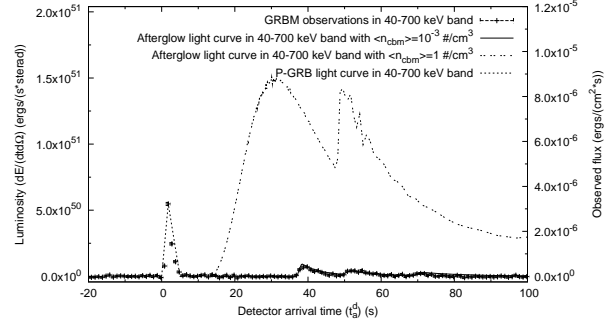

FIGURE 4. The theoretical fit of the *Beppo*SAX GRBM observations (solid line, see Fig. 3) is compared with the afterglow light curve in the 40–700 keV energy band obtained rescaling the CBM density to $\langle n_{cbm} \rangle = 1$ particle/cm^3 keeping constant its shape and the values of the fundamental parameters of the theory $E_{e^\pm}^{tot}$ and *B* (double dotted line). The P-GRB duration and luminosity (dotted line), depending only on $E_{e^\pm}^{tot}$ and *B*, are not affected by this process of rescaling the CBM density. Details in Bernardini et al. [3].
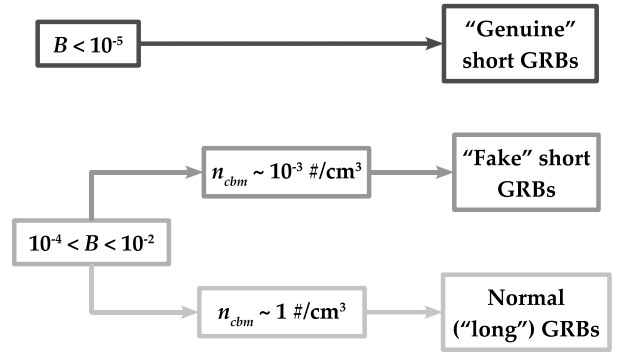

FIGURE 5. A sketch summarizing the different possibilities predicted by the "canonical GRB" scenario depending on the fireshell baryon loading *B* and the average CBM density $\langle n_{cbm} \rangle$.

minosity is lower than the P-GRB one, even if the afterglow total time-integrated luminosity is higher. This deflated afterglow peak can be observed as a "soft bump" following the P-GRB spike, as in GRB 970228 (Bernardini et al. [3, 4]), GRB 060614 (Caito et al. [10]), and the sources analyzed by Norris & Bonnell [19].

A sketch of the different possibilities depending on the fireshell baryon loading *B* and the average CBM density $\langle n_{cbm} \rangle$ is given in Fig. 5.

Before concluding, we turn to the Amati relation (Amati et al. [2], Amati [1]) between the isotropic equivalent energy emitted in the prompt emission E_{iso} and the peak energy of the corresponding time-integrated spectrum E_p. It clearly follows from our treatment (Bernardini et al. [5], Ruffini et al. [28, 22]) that both the hard-

to-soft behavior and the Amati relation occurs uniquely in the afterglow phase which, in our model, encompass as well the prompt emission. The observations that the initial spikelike emission in the above mentioned "fake" short GRBs, which we identify with the P-GRBs, as well as all "genuine" short GRBs do not fulfill the Amati relation (see Amati [1]) is indeed a confirmation of our theoretical model (see also Bernardini et al. [4]). We look forward to verifications in additional sources.

REFERENCES

1. Amati, L. 2006, MNRAS, 372, 233.
2. Amati, L., Frontera, F., Tavani, M., et al. 2002, A&A, 390, 81.
3. Bernardini, M.G., Bianco, C.L., Caito, L., et al. 2007, A&A, 474, L13.
4. Bernardini, M.G., Bianco, C.L., Caito, L., et al. 2007, AIP Conf. Proc., in this same volume.
5. Bernardini, M.G., Bianco, C.L., Chardonnet, P., et al. 2005, ApJ, 634, L29.
6. Bianco, C.L., Ruffini, R. 2004, ApJ, 605, L1.
7. Bianco, C.L., Ruffini, R. 2005, ApJ, 620, L23.
8. Bianco, C.L., Ruffini, R. 2005, ApJ, 633, L13.
9. Bianco, C.L., Ruffini, R., Xue, S.S. 2001, A&A, 368, 377.
10. Caito, L., Bernardini, M.G., Bianco, C.L., et al. 2007, AIP Conf. Proc., in this same volume.
11. Dainotti, M.G., Bernardini, M.G., Bianco, C.L., et al. 2007, A&A, 471, L29.
12. Della Valle, M., Chincarini, G., Panagia, N., et al. 2006, Nature, 444, 1050.
13. Dezalay, J.P., Barat, C., Talon, R., et al. 1992, AIP Conf. Proc. 265, 304.
14. Gal-Yam, A., Fox, D.B., Price, P.A., et al. 2006, Nature, 444, 1053.
15. Gehrels, N., Norris, J.P., Mangano, V., et al. 2006, Nature, 444, 1044.
16. Klebesadel, R.W. 1992, in "Gamma-ray bursts", CUP, p. 161.
17. Mangano, V., Holland, S.T., Malesani, D., et al. 2007, A&A, 470, 105.
18. Mészáros, P. 2006, Rep.Prog.Phys., 69, 2259.
19. Norris, J.P, Bonnell, J.T., 2006, ApJ, 643, 266.
20. Piran, T. 2004, Rev. Mod. Phys., 76, 1143.
21. Ruffini, R., Bernardini, M.G., Bianco, C.L., et al. 2005, AIP Conf. Proc. 782, 42.
22. Ruffini, R., Bernardini, M.G., Bianco, C.L., et al. 2006, ApJ, 645, L109.
23. Ruffini, R., Bernardini, M.G., Bianco, C.L., et al. 2007, AIP Conf. Proc. 910, 55.
24. Ruffini, R., Bianco, C.L., Chardonnet, P., et al. 2001, ApJ, 555, L107.
25. Ruffini, R., Bianco, C.L., Chardonnet, P., et al. 2001, ApJ, 555, L113.
26. Ruffini, R., Bianco, C.L., Chardonnet, P., et al. 2002, ApJ, 581, L19.
27. Ruffini, R., Bianco, C.L., Chardonnet, P., et al. 2003, AIP Conf. Proc. 668, 16.
28. Ruffini, R., Bianco, C.L., Chardonnet, P., et al. 2004, IJMPD, 13, 843.
29. Ruffini, R., Bianco, C.L., Chardonnet, P., et al. 2005, IJMPD, 14, 97.
30. Ruffini, R., Fraschetti, F., Vitagliano, L., Xue, S.S., 2005, IJMPD, 14, 131.
31. Ruffini, R., Salmonson, J.D., Wilson, J.R., Xue, S.S. 2000, A&A, 359, 855.